WAVELET-BASED CONTOURLET TRANSFORM AND ITS APPLICATION TO IMAGE CODING

Ramin Eslami and Hayder Radha

ECE Department, Michigan State University, East Lansing, MI 48824, USA

ABSTRACT

In this paper, we first propose a new family of geometrical image transforms that decompose images both radially and angularly. Our construction comprises two stages of filter banks that are non-redundant and perfect reconstruction and therefore lead to an overall non-redundant and perfect reconstruction transform. Using the wavelet transform as the first stage, we apply directional filter banks to the wavelet coefficients in such a way to maintain the anisotropy scaling law. Furthermore, we propose a new image coding scheme based on the proposed transform, the wavelet-based contourlet transform (WBCT), using a new contourlet-based set partitioning in hierarchical trees (CSPIHT) algorithm that provides an embedded code. Due to differences in parent-child relationships between the WBCT coefficients and wavelet coefficients, under CSPIHT, we developed an elaborated repositioning algorithm for the WBCT coefficients in such a way that we could scan spatial orientation trees that are similar to the original SPIHT algorithm. Our experiments demonstrate that the proposed approach is efficient in coding images that possess mostly textures and contours. Our simulation results also show that this new coding approach is competitive to the wavelet coder in terms of the PSNR-rate curves, and is visually superior to the wavelet coder for the mentioned images.

1. INTRODUCTION

Although the wavelet transform has been proven to be powerful in many signal and image processing applications such as compression, noise removal, image edge enhancement, and feature extraction; wavelets are not optimal in capturing the two-dimensional singularities found in images. Therefore, several transforms have been proposed for image signals that have incorporated directionality and multiresolution and hence, could more efficiently capture edges in natural images. Steerable pyramid [12], curvelets [1] and contourlets [3] are some popular examples. The contourlet transform is one of the new geometrical image transforms, which can efficiently represent images containing contours and textures [2][3]. This transform uses a structure similar to that of curvelets [1], that is, a stage of subband decomposition followed by a directional transform. In the contourlet transform, a Laplacian pyramid is employed in the first stage, while directional filter banks (DFB) are used in the angular decomposition stage. Due to the redundancy of the Laplacian pyramid, the contourlet transform has a redundancy factor of 4/3 and hence, it may not be the optimum choice for image coding applications. Recently, some approaches have been attempted to introduce non-redundant image transforms based on the DFB with the capability of both radial and angular decomposition. The octave-band directional filter banks [4] are a new family of directional filter banks that offer an octave-band radial decomposition as well. Another approach is the critically sampled contourlet (CRISP-contourlet) transform [6], which is realized using a one-stage non-separable filter bank. Using similar frequency decomposition to that of the contourlet transform, it provides a non-redundant version of the contourlet transform.

In this paper we first propose a new non-redundant image transform, the *Wavelet-Based Contourlet Transform* (WBCT), with a construction similar to the contourlet transform. Then, we use the non-redundant WBCT in conjunction with an SPIHT-like algorithm [10] to construct an embedded image coder. Due to differences in parent-child relationships between the WBCT coefficients and wavelet coefficients, we develop an elaborated repositioning algorithm for the WBCT coefficients in such a way that we could have similar *spatial orientation trees* [10] (the *zero-trees* introduced in [11]) as the ones used for scanning the wavelet coefficients. We refer to our contourlet-based, SPIHT-like scanning as *CSPIHT*. Our simulation results show that the proposed coder is competitive to the original SPIHT coder in terms of the PSNR values, especially for a category of images that have a significant amount of textures and oscillatory patterns and therefore are not "wavelet-friendly" images and is visually superior to the SPIHT coder for the mentioned images.
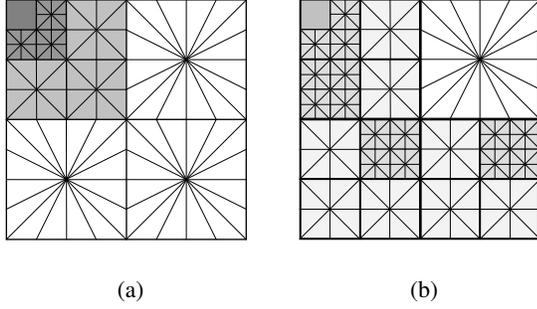
Fig. 1. (a) A schematic plot of the WBCT using 3 dyadic wavelet levels and 8 directions at the finest level ($N_D = 8$). The directional decomposition is overlaid the wavelet subbands. (b) An example of the wavelet-based contourlet packet.

Fig. 2. A diagram that shows the multiresolutional subspaces for the WBCT.

2. THE WBCT CONSTUCTION

Similar to the contourlet transform, the WBCT consists of two filter bank stages. The first stage provides subband decomposition, which in the case of the WBCT is a wavelet transform, in contrast to the Laplacian pyramid used in contourlets. The second stage of the WBCT is a directional filter bank (DFB), which provides angular decomposition. The first stage is realized by separable filter banks, while we implement the second stage using non-separable filter banks. For the DFB stage, we employ the iterated tree-structured filter banks using fan filters [2].

At each level (*j*) in the wavelet transform, we obtain the traditional three highpass bands corresponding to the LH, HL, and HH bands. We apply DFB with the same number of directions to each band in a given level (*j*). Starting from the desired maximum number of directions $N_D = 2^L$ on the finest level of the wavelet transform *J*, we decrease the number of directions at every other dyadic scale when we proceed through the coarser levels ($j < J$). This way, we could achieve the anisotropy scaling law; that is $width \approx length^2$.

Fig. 1(a) illustrates a schematic plot of the WBCT using 3 wavelet levels and $L = 3$ directional levels. Since we have mostly vertical directions in the HL image and horizontal directions in the LH image, it might seem logical to use partially decomposed DFB's with vertical and horizontal directions on the HL and LH bands, respectively. However, since the wavelet filters are not perfect in splitting the frequency space to the lowpass and highpass components, that is, not all of the directions in the HL image are vertical and in the LH image are horizontal, we use fully decomposed DFB on each band.

One of the major advantages of the WBCT is that we can have *Wavelet-based Contourlet Packets* in much the same way as we have Wavelet Packets. That is, keeping 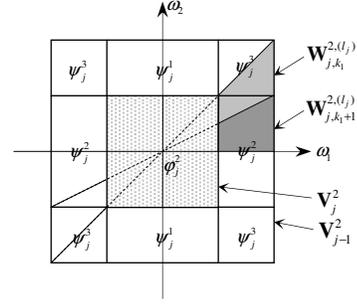in mind the anisotropy scaling law (the number of directions is doubled at every other wavelet levels when we refine the scales), we allow quad-tree decomposition of both lowpass and highpass channels in wavelets and then apply the DFB on each subband. Fig. 1(b) schematically illustrates an example of the wavelet-based contourlet packets. However, if the anisotropy constraint were ignored, a quad-tree like angular decomposition, which is introduced in [9] as *Contourlet Packets*, can be constructed as well. Below, we present a brief multiresolution analysis of the WBCT.

Following a similar procedure outlined in [3], for an *l*-level DFB we have 2^l directional subbands with $G_k^{(l)}$, $0 \le k < 2^l$ equivalent synthesis filters and the overall downsampling matrices of $S_k^{(l)}$, $0 \le k < 2^l$ defined as:

$$S_k^{(l)} = \begin{cases} \begin{bmatrix} 2^{l-1} & 0 \\ 0 & 2 \end{bmatrix}, & if \quad 0 \le k < 2^{l-1} \\ \begin{bmatrix} 2 & 0 \\ 0 & 2^{l-1} \end{bmatrix}, & if \quad 2^{l-1} \le k < 2^l \end{cases}.$$

Then, $\{g_k^l[n - S_k^{(l)}m]\}$, $0 \le k < 2^l$, $m \in \mathbb{Z}^2$, is a directional basis for $l^2(\mathbb{Z}^2)$; where $g_k^{(l)}$ is the impulse response of the synthesis filter $G_k^{(l)}$. Assuming an orthonormal separable wavelet transform, we will have separable 2-D multiresolution [7]:

$$\mathbf{V}_j^2 = \mathbf{V}_j \otimes \mathbf{V}_j, \qquad and \qquad \mathbf{V}_{j-1}^2 = \mathbf{V}_j^2 \oplus \mathbf{W}_j^2,$$

where $\mathbf{W}_j^2$ is the detail space and orthogonal component of $\mathbf{V}_j^2$ in $\mathbf{V}_{j-1}^2$. The family $\{\psi_{j,n}^1, \psi_{j,n}^2, \psi_{j,n}^3\}_{n \in \mathbb{Z}^2}$ is an orthonormal basis of $\mathbf{W}_j^2$. Now, if we apply l_j directional levels to the detail multiresolution space $\mathbf{W}_j^2$, we obtain 2^{l_j} directional subbands of $\mathbf{W}_j^2$ (see Fig. 2):

$$\mathbf{W}_j^2 = \overset{2^{l_j}-1}{\underset{k=0}{\oplus}} \mathbf{W}_{j,k}^{2,(l_j)},$$
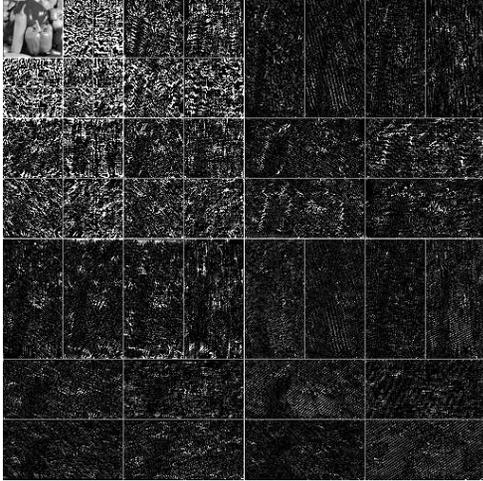
Fig. 3. The WBCT coefficients of the *Peppers* image.
For better visualizing, the transform coefficients are
clipped between 0 and 7.

Defining

$$\eta_{j,k,n}^{i,(l_j)} = \sum_{m \in \mathbb{Z}^2} g_k^{l_j}[m - S_k^{(l_j)} n] \psi_{j,m}^i, \qquad i = 1, 2, 3,$$

the family $\{\eta_{j,k,n}^{1,(l_j)}, \eta_{j,k,n}^{2,(l_j)}, \eta_{j,k,n}^{3,(l_j)}\}_{n \in \mathbb{Z}^2}$ is a basis for the

subspace $\mathbf{W}_{j,k}^{2,(l_j)}$.

Fig. 3 shows an example of the WBCT coefficients of
the *Peppers* image. Here we used 3 wavelet levels and 8
directions at the finest level. You can see that most of the
coefficients in the HL subbands are in the vertical
directional subbands (the upper half of the subbands)
while those in the LH subbands are in the horizontal
directional subbands (the lower half of the subbands).

3. WBCT CODING USING THE CSPIHT ALGORITHM

Said and Pearlman [10] developed the SPIHT algorithm
for wavelet coding of images and could achieve significant
improvement over the EZW coder [11][5]. Similar to the
spatial orientation tree (*or* zero-tree) concept of wavelet
coefficients in which we have a parent-child relationship
along wavelet scales, one can find parent-child
dependencies in other subband systems. In the case of the
contourlet transform, one can assume two different parent-
child relationships depending on the number of directional
decompositions in the contourlet subbands [9]. If the two
successive scales in which the parent and children lie have
the same number of directional decompositions, then the
parent and children would lie in the corresponding
directional subbands; however if the scale in which the
children lie has twice as many directional subbands as the
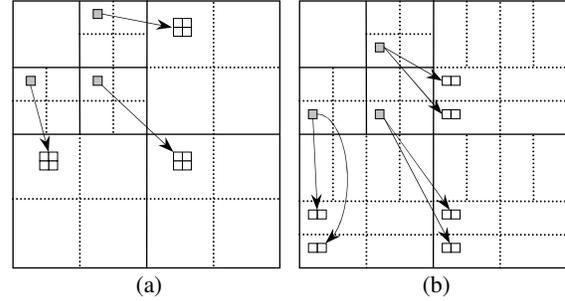

(a)   (b)

Fig. 4. Two possible parent-child relationships in the WBCT.
Wavelet subbands (or radial subbands in the WBCT) are
separated by the solid lines and directional subbands are
separated by the dotted lines. (a) When the number of directional
subbands are the same at the two wavelet scales. Here we have 4
directions at each wavelet subband. (b) When the number of
directional subbands in the finer wavelet scale (here is 8) is
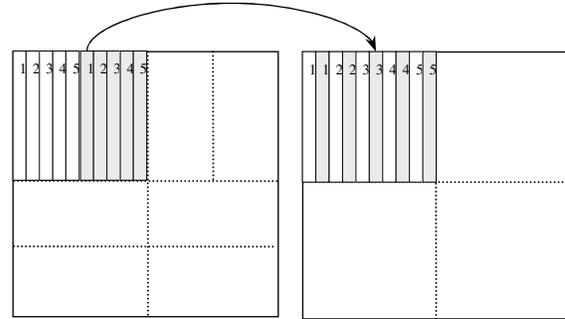twice as many as those in the coarser wavelet scale (here is 4).

Fig. 5. An example of repositioning a radial subband in the
WBCT having 8 directional subbands assuming its coarser
subband is at first level and has 4 directional decompositions. In
this process we combine each two adjacent directional subbands
by interlacing the columns of horizontal directional subbands
(upper half subbands) and the rows of vertical directional
subbands (lower half subbands).

scale in which the parent lies, the four children will be in
two adjacent directional subbands. These two directional
subbands correspond to the directional decomposition of
the directional subband in which the parent is located. Due
to the similarities of the WBCT to the contourlet
transform, for each LH, HL, and HH subband we can
assume the same parent-child relationships as illustrated in
Fig. 4. Therefore, due to differences in parent-children
dependencies between the WBCT and the wavelet
transform, before applying the SPIHT algorithm, we
reposition the transform coefficients in the WBCT in such
a way to be able to use a similar SPIHT algorithm. Fig. 5
shows an example of repositioning a radial subband in the
WBCT having 8 directional decompositions. In the next
section, we show the experimental results obtained for
images that mostly contain contours and oscillatory
patterns such as textures (from *Brodatz* texture images
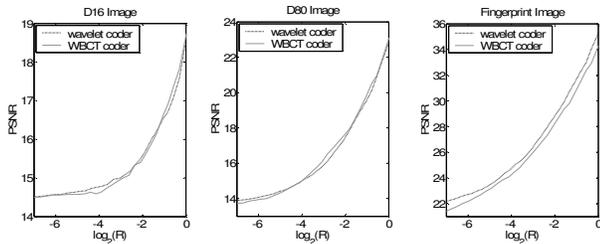collection) and fingerprint images.

Fig. 6. Rate-distortion curves obtained for the images *D16, D80* and *Fingerprint* using the SPIHT and CSPIHT coders.

4. NUMERICAL EXPERIMENTS

We tested the proposed WBCT/CSPIHT coding scheme as well as the original wavelet-based SPIHT coder on several images such as textures and fingerprints, each having a size of 512x512. The WBCT uses 5 wavelet levels and 16 directions at the finest scale. We used non-separable fan filters of support sizes (23, 23) and (45, 45) as described in [8]. The FIR half-band filter used for constructing fan filters is designed using the *"remez"* function in MATLAB. We used biorthogonal Daubechies 9-7 wavelets in both schemes. We used an arithmetic encoder to entropy-code the resulting bit streams of the SPIHT algorithm. Fig. 6 shows some of the rate-distortion curves obtained for coding the images using the SPIHT wavelet and WBCT coders. We can see that the PSNR values for both schemes are comparable. However, our experiments indicated that the proposed scheme is superior in preserving textures and details in the coded images. This observation is not effectively captured by the PSNR metric. Fig. 7 shows the visual coded results of the *Fingerprint, D80*, and a part of the *Barbara* images. As seen, more ridges in the coded *Fingerprint* image by the proposed coder are retained. This figure also clearly shows the capability of the proposed coder for images consisting of mainly textures and oscillatory patterns.

5. CONCLUSION

We proposed the wavelet-based contourlet transform, which is a new non-redundant transform, and designed a new image coder based on the proposed WBCT transform using an SPIHT-like algorithm. Our simulation results indicated that the proposed coder is visually superior to the wavelet SPIHT scheme in preserving details and textures in the coded images.

6. REFERENCES

[1] E. J. Candes and D. L. Donoho, "Curvelets – a suprizingly effective nonadaptive representation for objects with edges," *in Curve and Surface Fitting*, Saint- Malo, 1999, Vanderbuilt Univ. Press.

[2] M. N. Do, *Directional multiresolution image representations.* PhD thesis, EPFL, Lausanne, Switzerland, Dec. 2001.
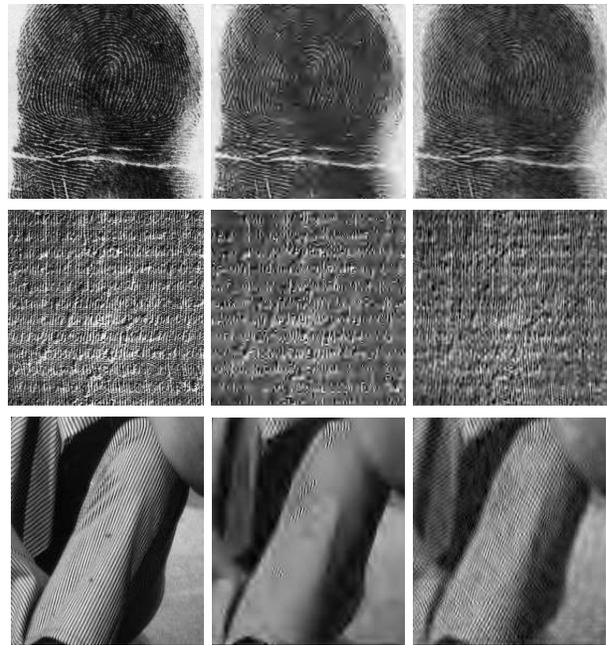
Fig. 7. The *Fingerprint* (top row), *D80* (middle row) and *Barbara (part of the image is shown)* (bottom row) images coded at a rate equal to 0.05, 0.05, and 0.1 bpp, respectively. *Left:* original. *Middle:* the SPIHT coder results. *Right:* the proposed CSPIHT coder results.

[3] M. N. Do and M. Vetterli, "Contourlets," in *Beyond Wavelets*, Academic Press, New York, 2003.

[4] P. Hong and M. J. T. Smith, "An octave-band family of non-redundant directional filter banks," *in IEEE proc. ICASSP,* vol. 2, pp. 1165-1168, 2002

[5] Image Communication Lab., UCLA, *Wavelet Image Coding: PSNR Results.* Available at http://www.icsl.ucla.edu/~ipl/psnr_results.html .

[6] Y. Lu and M. N. Do, "CRISP-contourlets: a critically sampled directional multiresolution image representation," *in proc. of SPIE conference on Wavelet Applications in Signal and Image Processing X*, San Diego, USA, August 2003.

[7] S. Mallat, *A Wavelet Tour of Signal Processing.* Academic Press, 2nd Ed., 1998.

[8] S. M. Phoong, C. W. Kim, P. P. Vaidyanathan, and R. Ansari, "A new class of two-channel biorthogonal filter banks and wavelet bases," *IEEE trans. on* **SP**, vol. 43, no. 3, pp. 649-665, Mar. 1995.

[9] D. D.-Y. Po and M. N. Do, "Directional multiscale modeling of images using the contourlet transform," submitted to *IEEE Trans. on Image Processing*, 2003.

[10] A. Said and W. A. Pearlman, "A New Fast and Efficient Image Codec Based on Set Partitioning in Hierarchical Trees," *IEEE Trans. on Circuits and Systems for Video Technology,* vol. 6, pp. 243-250, June 1996.

[11] J.M. Shapiro, "Embedded image coding using zerotrees of wavelet coefficients," *IEEE Trans. on Signal Processing*, vol. 41, pp. 3445-3462, Dec. 1993.

[12] E. P. Simoncelli and W. T. Freeman, "The steerable pyramid: A flexible architecture for multi-scale derivative computation" *in proc. ICIP,* Washington DC, 1995.